Singlet Energy Dissipation in the Photosystem II Light-Harvesting Complex Does Not Involve Energy Transfer to Carotenoids

Mueller, Marc G.; Lambrev, Petar; Reus, Michael; Wientjes, Emilie; Croce, Roberta; Holzwarth, Alfred R.; Müller, Marc G.

Published in:
Chemphyschem

DOI:
10.1002/cphc.200900852

DOI: 10.1002/cphc.200900852

Singlet Energy Dissipation in the Photosystem II Light-Harvesting Complex Does Not Involve Energy Transfer to Carotenoids

Marc G. Müller,[a] Petar Lambrev,[a] Michael Reus,[a] Emilie Wientjes,[b] Roberta Croce,[b] and Alfred R. Holzwarth*[a]

The energy dissipation mechanism in oligomers of the major light-harvesting complex II (LHC II) from *Arabidopsis thaliana* mutants *npq1* and *npq2*, zeaxanthin-deficient and zeaxanthin-enriched, respectively, has been studied by femtosecond transient absorption. The kinetics obtained at different excitation intensities are compared and the implications of singlet–singlet annihilation are discussed. Under conditions where annihilation is absent, the two types of LHC II oligomers show distributive biexponential (bimodal) kinetics with lifetimes of ≈5–20 ps and ≈200–400 ps having transient spectra typical for chlorophyll excited states. The data can be described kinetically by a two-state compartment model involving only chlorophyll excited states. Evidence is provided that neither carotenoid excited nor carotenoid radical states are involved in the quenching mechanism at variance with earlier proposals. We propose instead that a chlorophyll–chlorophyll charge-transfer state is formed in LHC II oligomers which is an intermediate in the quenching process. The relevance to non-photochemical quenching in vivo is discussed.

1. Introduction

The performance and survival of plants in natural environments relies on their ability to actively adapt to severely changing light conditions. The photosynthetic machinery attempts to avoid radiation damage in excess light by modulating the efficiency of light harvesting and the delivery of excitation energy to the reaction centers through a number of mechanisms commonly termed as "non-photochemical quenching" (NPQ) (for recent reviews see refs. [1–3]). A large amount of evidence has been accumulated that the major light-harvesting complex (LHC II) of Photosystem II (PSII) is one of the active components of NPQ.[4–6] It is well established that the activation of NPQ depends on the ΔpH across the thylakoid membrane,[7–9] the de-epoxidation of the xanthophyll cycle pigments, that is, the conversion of violaxanthin (Vx) to antheraxanthin and zeaxanthin (Zx),[10] and the action of the PsbS protein.[11,12] Quite generally, it is assumed that carotenoids (Cars) play a direct role in the quenching. However, the exact mechanism(s) by which these factors interplay has remained a long-standing matter of debate and a number of alternative models exist at present,[2,6] for reviews see refs. [13–15]. The finding that oligomerization of isolated LHC II by detergent removal in vitro results in a drastic decrease of the fluorescence yield and lifetime[16,17] has led to the suggestion that a similar quenching mechanism may be responsible for NPQ in vivo, and in particular for the fast qE-quenching phase of NPQ[18,19] despite the fact that neither PsbS nor Zx is present in these oligomers. Consequently, oligomerized LHC II has been proposed to provide a good in vitro model for elucidating the qE-quenching mechanism in vivo. It has been demonstrated for example, that both in the quenched state in vivo and in oligomerized LHC II the conformation of the carotenoid neoxanthin (Nx) is modified in a similar manner.[20] It has been shown further that qE quenching both in vivo and quenching in oligomerized LHC II in vitro is associated with the appearance of a pronounced far-red (FR) fluorescence component with lifetimes in the order of a few 100 ps.[21,22]

In the LHC II quenching hypothesis non-radiative deactivation of the excitations (NPQ) is assumed to arise due to a conformational change or switch resulting in the formation of quenching centers[23,24] that might be established either between chlorophylls (Chls) or between Chl and xanthophylls located within individual or adjacent trimeric complexes. Several hypotheses for the nature of these interactions have been raised starting from a simple concentration effect to more specific models addressing particular pigments in LHC II. The model of Pascal et al.[25] for the quenching in LHC II crystals assumes that energy dissipation occurs in a Chl dimer, or excimer, formed by a conformational switch within a LHC II monomer subunit that changes the interaction of Chls with a nearby carotenoid pigment. Based on femtosecond transient absorption (TA) data on LHC II aggregates[20] it has been proposed

[a] Dr. M. G. Müller, Dr. P. Lambrev, M. Reus, Prof. Dr. A. R. Holzwarth
Max-Planck-Institut für Bioanorganische Chemie
Stiftstraße 34-36, 45470 Mülheim an der Ruhr (Germany)
Fax: (+49) 208-306-3951
E-mail: Holzwarth@mpi-muelheim.mpg.de

[b] Dr. E. Wientjes, Prof. Dr. R. Croce
University of Groningen, Department of Biophysical Chemistry
Groningen Biomolecular Sciences and Biotechnology Institute
Groningen (The Netherlands)

Supporting information for this article is available on the WWW under http://dx.doi.org/10.1002/cphc.200900852.

that the quenching is initiated by a conformational change in LHC II which enhances the rate of singlet excitation energy transfer from Chl to lutein 1 (Lut1). In this model, Chl excited-state quenching occurs by energy transfer to Lut1 with a lifetime of about 200 ps, followed by rapid deactivation (ca. 8 ps) of the S_1 state of Lut1. In other models incorporating the direct role of xanthophylls in the quenching mechanism, the energy is captured by Zx via a singlet–singlet transfer (gear-shift model[26,27]) or by the formation of a radical pair in a Chl–Zx heterodimer.[28] The latter mechanism has been proposed to occur primarily in minor LHCs[29,30] but has been excluded for the major LHC II complex.

We recently showed that in the fluorescence kinetics of isolated LHC II oligomers, energy is trapped rapidly (with lifetime ranging from ca. 5–20 ps) on a new Chl excited state—proposed to be an emissive charge-transfer (CT) state—from which relatively slow deactivation occurs (200–400 ps).[21] The exact mechanism of decay, particularly whether it proceeds directly to the ground state or via further intermediate steps, for example, involving Cars, could not be determined from the fluorescence data. For this reason, we have now studied the ultrafast dynamics in LHC II oligomers by femtosecond transient absorption (TA). We specifically compared LHC II oligomers isolated from the *Arabidopsis thaliana* mutants *npq1* and *npq2*,[31] which differ in their xanthophyll content, to test for a possible role of Zx in the quenching mechanism. The *npq1* LHC II contains no Zx whereas *npq2* LHC II has the V1 site occupied by Zx. Our study specifically tests the conformational switch model by Ruban et al.[20] and aims to clarify the possible role of Cars in the quenching of LHC II oligomers. Special attention was paid on obtaining data under annihilation-free conditions. We show that dissipation of Chl* excitation does not directly involve energy transfer to Cars and we discuss the relevance of our findings for the in vivo NPQ process.

Experimental Section

Major LHC II (LHC IIb) trimers were isolated from leaves of the *Arabidopsis thaliana* mutants *npq1* and *npq2* by sucrose density gradient centrifugation of thylakoids solubilised with 0.6% α-dodecylmaltoside.[32] According to the pigment analysis, performed as described in ref. [33], trimers of *npq1* contained 2.5 mol Lut, 0.3 mol Vx, and 1 mol Nx per monomer, but no Zx, and LHC II isolated from the *npq2* mutant contained 2.4 mol Lut and 1.2 mol Zx. Aggregates of LHC II were produced by incubating the trimers with 250 mg mL^{-1} BioBeads SM-2 (Bio-Rad) to remove the detergent. Aggregation was monitored by the decrease of the fluorescence yield and increase of the scattering of the sample and confirmed by the appearance of a 700 nm band in the fluorescence spectra registered at 77 K.[21]

Room-temperature femtosecond transient absorption measurements were performed using a setup described earlier.[34] In brief, pulses from a Ti:Sa laser system, regeneratively amplified to about 0.5 mJ, 70–80 fs FWHM at 3 kHz repetition rate were used to generate white light probe pulses and, via an optical parametric oscillator, pump pulses at 680 nm with approximately 10 nm width and 70 fs pulse duration were generated. The pump pulses were attenuated to $7{\cdot}10^{12}$–$1.4{\cdot}10^{14}$ photons cm^{-2} pulse^{-1}) and focused to a 130 μm diameter spot. The sample of OD 6–8 per cm at the excitation wavelength was contained in a vertically and horizontally moved cuvette with optical path length of 1 mm. The transient absorption changes were detected at magic angle polarization in two delay time ranges (namely, 13 and 500 fs per point) over 20 ps and 800 ps, respectively, total delay by a spectrograph/fast diode array camera system covering a wavelength range of 125 nm per recording at 0.5 nm resolution.

The TA data were analyzed by the lifetime density method applied in our laboratory[34] using a distribution of up to 100 exponential functions with lifetimes ranging up to 4 ns to fit the data globally in the time and wavelength domain using an inverse Laplace transform together with deconvolution with the excitation pulse. The resulting lifetime density maps (LFD maps) represent the measured kinetics without any prior assumptions of the underlying kinetic scheme. Kinetic compartment modeling was performed (so-called target analysis[35]) based on the data obtained from the lifetime density analysis.

2. Results

2.1 Absorption Kinetics at Different Excitation Intensities

Figure 1 shows the lifetime density maps resulting from femtosecond TA measurements on LHC II oligomers from *npq2*, registered at four different laser intensities, corresponding to photon densities of about $7{\cdot}10^{12}$, $2.5{\cdot}10^{13}$, $4.5{\cdot}10^{13}$, and $1.4{\cdot}10^{14}$ photons cm^{-2} pulse^{-1} (Figs. 1 A–D, respectively). At the lowest excitation intensity, the data reveal two negative amplitude components with lifetimes centered around 4 and 200 ps. At all excitation intensities, the lifetimes are substantially distributed. At increasing photon densities the two lifetime distributions are broadened further. Concomitantly with increasing intensity the centers of the lifetime distributions are shifted to shorter lifetimes due to pronounced excited state annihilation. At the highest intensity the bleaching recovery kinetics consists of a quasi-continuum of lifetimes covering the range from <1 to 500 ps. At the higher intensities also two positive components (rise of bleaching) of very small amplitude become visible—a $\approx$3 ps component in the Chl *b* or short Chl *a* range (660 nm) and also a long lifetime exceeding the measured range (>3 ns) is observed. The broadening of the lifetime distributions at increasing intensity cannot be accounted for by inaccuracies in the data analysis. On the contrary, the lifetimes are expected to be more precisely determined (i.e. narrowing of the distributions) with the higher signal-to-noise ratio achieved at higher laser intensities.[34] The appearance of new and shorter-lived components is clearly linked to singlet–singlet annihilation processes in the sample. It is evident that annihilation tremendously complicates the overall kinetics and hence also hampers or even renders impossible any detailed kinetic modeling. Thus obtaining data free of annihilation is a prerequisite for a meaningful and reliable kinetic modeling. The excitation condition in Figure 1 A is clearly annihilation-free and under the conditions of Figure 1 B the annihilation limit is just reached, that is, annihilation is just starting to set in (see Figure S2 of the Supporting Information).

Figures S1 A–C of the Supporting Information show the original kinetic traces at the highest excitation energy used by us

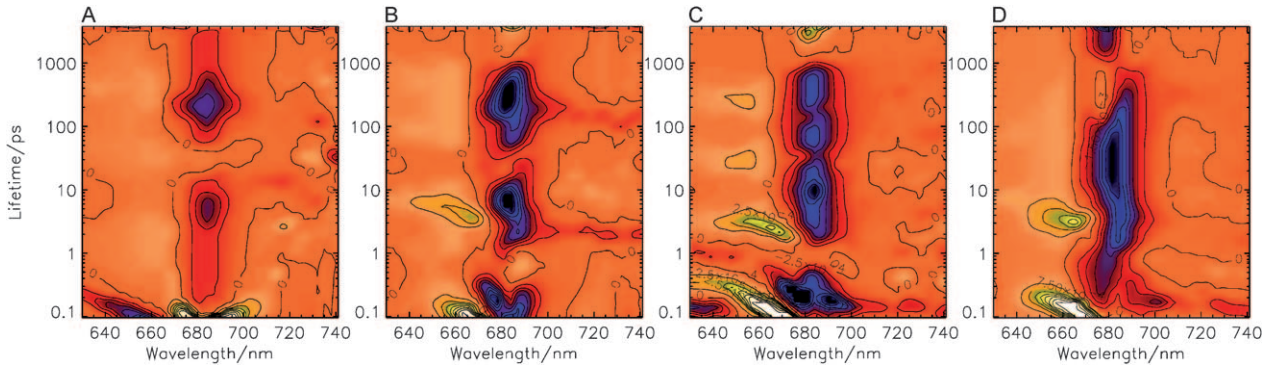

Figure 1. Lifetime density maps for the transient absorption kinetics of LHC II oligomers of *Arabidopsis npq2* measured at different excitation rates: A) $7{\cdot}10^{12}$, B) $2.5{\cdot}10^{13}$, C) $4.5{\cdot}10^{13}$, D) $1.4{\cdot}10^{14}$ photons cm^{-2} $pulse^{-1}$. The lifetime scale is logarithmic and the amplitudes are color-coded, where red denotes zero level, yellow to white: positive amplitude (meaning either rise of bleaching or decay of ESA), and blue to black: negative amplitude (decay of bleaching or rise of ESA).

(i.e. $1.4{\cdot}10^{14}$ photons cm^{-2} $pulse^{-1}$, Figure 1 D) at various wavelengths for comparison. To achieve simpler kinetics with much fewer kinetic components—thus allowing to unequivocally determine the rates intrinsic to the system over the whole wavelength range of interest, including the blue range where carotenoid signals are expected to show up—it is necessary to avoid any substantial singlet–singlet annihilation and to keep identical excitation conditions over the whole detected wavelength range. The very small signal strength in the blue range prevents measurements over the whole wavelength range of interest at the conditions of Figure 1 A. However, our experiments as well as the annihilation estimates (see Supporting Information) indicate that at $2.4{\cdot}10^{13}$ photons cm^{-2} $pulse^{-1}$—that is, at an intensity slightly below that of Figure 1 B—data can be acquired also in the blue (Car) wavelength range with a very good signal-to-noise ratio without any significant annihilation contribution (see below).

2.2 Transient Absorption Spectra under Low Annihilation Conditions

The lifetime density maps obtained at nearly annihilation-free conditions are presented in Figure 2 for LHC II oligomers prepared from *npq1* and *npq2* LHC II trimers. Transient spectra at several selected times (deconvoluted by the excitation pulse) are also given. The two mutants show virtually the same kinetics, very similar to the one shown in Figure 1 A. The main bleaching at 682 nm decays with lifetimes centered at 4 and 200 ps. Even at annihilation-free conditions (see Figures 1 A and 2 A, B) the lifetimes are not sharply defined but distributed over a relatively wide range, for example, the longer-lived component covers a lifetime interval of about 100–500 ps and the short-lived component is distributed over 2–10 ps. This behavior must be attributed to some intrinsic kinetic heterogeneity. It could either derive from a structural heterogeneity of the oligomers leading to distribution in the strength of the pigment interactions or to some intrinsic heterogeneity in the nature of the quenching process. It is important to note here, however, that there occurs no spectral heter-

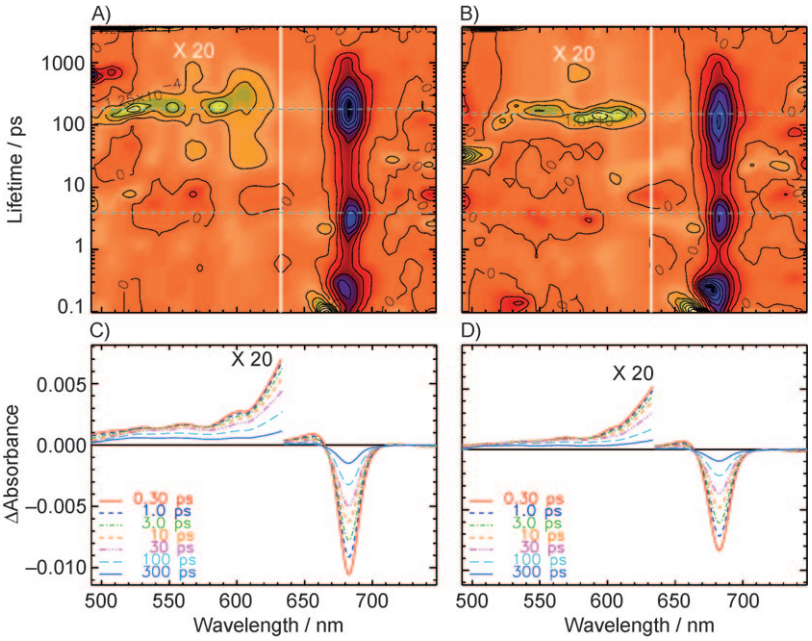

Figure 2. Lifetime density maps (A, B) and corresponding transient absorption difference spectra at different delay times (C, D) for LHC II oligomers of *Arabidopsis npq1* (A, C) and *npq2* (B, D). The data are obtained at $2.4{\cdot}10^{13}$ photons cm^{-2} $pulse^{-1}$. Note that the absorption difference in the blue range is multiplied by 20. Note: In this type of representation of the transient absorption data, negative peaks (in dark blue) stand for decay of the GSB or rise of ESA and, reciprocally, positive peaks (in yellow) mean decay of ESA or rise of GSB (for further details see ref. [34]).

ogeneity in these distributions, that is, the difference spectra within each of the two distributions are essentially homogeneous.

Examination of the blue-wavelength range reveals a rather broad and featureless absorption band that also decays with a lifetime distribution centered at 200 ps, similar to the main bleaching signal in the red spectral range. The signal amplitude in this wavelength range is quite small—less than 2% of the main bleaching amplitude in the Chl Q_y region. The difference spectra in the blue range are reminiscent of the TA spectral shape of excited Chls rather than for Cars, since Cars have relatively narrow (≈20–30 nm wide) S_1 absorption bands.[34] Interestingly, no significant rise terms (negative amplitude) can be seen in the blue-wavelength range (Figure 2 A, B). To verify the absence of any rise components we also examined the raw kinetic traces in this wavelength region (see Figure S5 of the Supporting Information). Considering that the pump pulse (680 nm) excites only Chls and not Cars, we can thus qualitatively assign the transient changes in the blue range solely to the decay of Chl excited states.

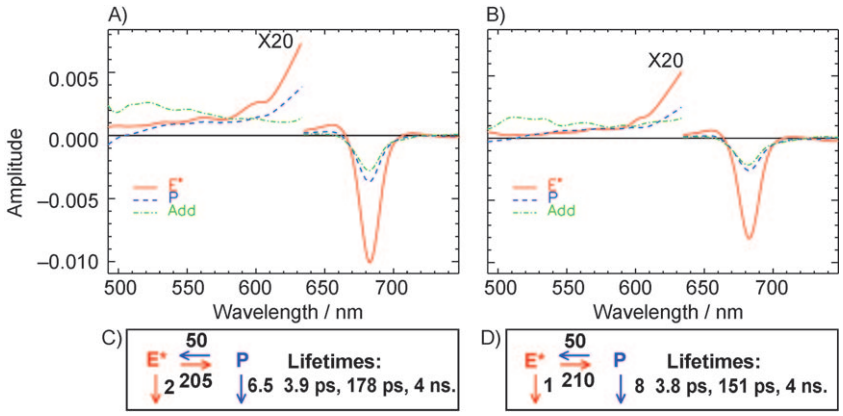

Figure 3. Species-associated absorption difference spectra (SADS) obtained from target analysis of the lifetime density data (shown in Figure 2) for oligomers of *npq1* (panel A) and *npq2* (panel B) using the fast/slow kinetic model represented in panels C and D. The numbers next to the arrows of the kinetic scheme are the rate constants of transfer/decay (in ns^{-1}) resulting from the kinetic analysis. The corresponding lifetimes of the kinetic schemes are also provided to the right. The >4 ns additional component of small amplitude corresponds either to a ^{3}Chl or a ^{3}Car; the lifetime is longer than our time range and was thus fixed.

2.3 Kinetic Modeling of the Transient Absorption Data

Global target analysis[35] was performed on the TA data. Ignoring the significant distribution of both lifetimes, the overall TA kinetics under low annihilation conditions is essentially bi-exponential (plus a very small amount of a long-lived ns component; Figure 2). There are two principal ways to describe such bi-exponential kinetics: In the simplest possible model the two lifetime components could behave completely independently (i.e. a model of two independently decaying states). Such a simple model does not give reasonable kinetic spectra and is also unlikely for mechanistic reasons because it precludes the formation of a quenching intermediate from the initially excited Chl states. A more reasonable model would be a connected two-state model, that is, the originally excited Chl state(s) (educt state E* in Figure 3) would convert into an intermediate state (product state P in Figure 3) which would then decay to the ground state. At this level, nothing particular needs to be assumed about the photophysical nature of the intermediate state or the process connecting the two states. In principle, either energy transfer, electron transfer or other processes would be possible a priori. There is one important point however: For formal mathematical reasons the biexponential kinetics resulting from such a model has two different mathematical solutions, both involving two excited states and/or intermediates. Both solutions have the same two lifetimes (i.e. they have identical eigenvalues for their kinetic matrices[35]) and will thus fit the bi-exponential data set in a mathematical sense equally well. However, only one of these solutions also represents a *physically reasonable* description of the kinetics. The important difference between the two solutions is in the sequence of the slow and fast steps, that is, they are reversed in the two models. We will thus call these two possible solutions the "fast/slow" and the "slow/fast" models depending on the relative rates of the first and second reaction steps. Despite having the same lifetimes the two models differ pronouncedly in their species-associated absorption difference spectra (SADS). Which one of the two mathematical solutions is the *physically reasonable* solution thus cannot be determined on the basis of the kinetics or the quality of the fit, but can only be judged based on the resulting SADS. It is thus essential to explicitly test both of these models on the kinetic data and then select the solution that gives the physically reasonable SADS.

Assuming for both models an initially excited state Chl state E* which converts into a product state P the kinetic results in terms of the rate constants and the SADS of the two models are shown in Figures 3 and 4, respectively, for the fast/slow and the slow/fast models. In the fast/slow model (Figure 3), a back reaction to the initially excited state was necessary when fitting the data, whereas in the slow/fast model (Figure 4), the back reaction rate was zero. This difference does not however change the bi-exponential nature of the kinetics of both models: The two mathematical solutions involve: i) a fast reaction step (energy transfer, electron transfer, etc.) from E* to P and a slow decay of P into another, ground or intermediate, state (Figure 3) and ii) a slow initial reaction step from E* to P, followed by a fast decay of P (Figure 4). To account for the very small (<5% amplitude) long-lived component in the TA, an additional component with a lifetime of about 4 ns lifetime has been included in the kinetic Scheme as well.

Figure 3 shows the results of fitting the "fast/slow" model to the TA data of *npq1* and *npq2* oligomers. The two LHCs from the two mutants show remarkably similar SADS. The spectrum

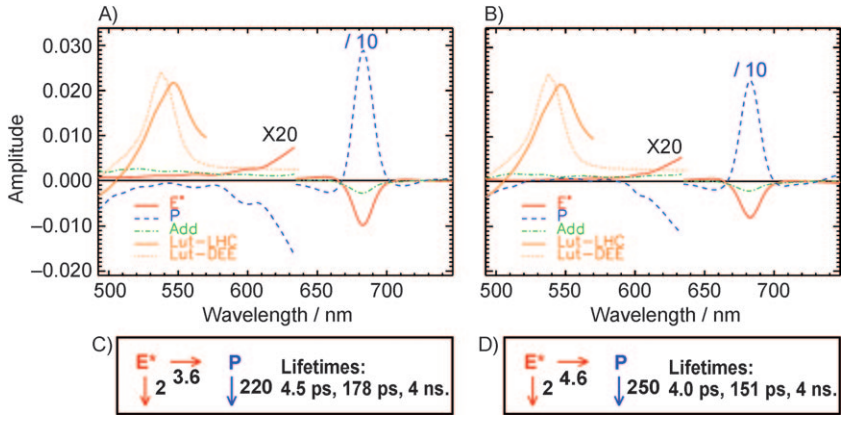

Figure 4. SADS (A, B) obtained from target analysis of the lifetime density data for oligomers (Figure 2) testing a kinetic model comprising slow transfer to the quencher P (assuming for example, a Car S_1 state[20]) followed by fast decay of P (slow/fast model). The kinetic model schemes are shown in panels (C) and (D). The numbers next to the arrows of the kinetic schemes are the rate constants of transfer/decay (in ns^{-1}) resulting from the kinetic analysis. The corresponding lifetimes of the kinetic scheme are also provided to the right. Orange curves: SADS of the Lut/diethylether S_1 excited state absorption (Lut-DEE) and the Lut S_1 absorption in LHC II monomers (Lut-LHC) for comparison.

of the first state (E*) can be clearly assigned to Chl ground-state bleaching (GSB). The overall shape of the spectrum in the Q_y range of the P state, having also a main bleaching band at 682 nm, indicates that it also corresponds to some type of Chl* state. However, this state shows significantly lower amplitude than the E* state. Moreover, the spectrum is broadened compared to the Chl* (E*) spectrum and the Q_y bleaching band features a broad tail extending to the red (see also Figure S7 of the Supporting Information). Since there is no absorption in the long-wavelength range, the negative long-wave signal can only be due to stimulated emission (SE), which is very pronounced in the SADS of the P state. This characterizes P as an excited state in this model. The modeling also shows that no further major product or intermediate state is formed from the P state (except for the very small amount of the long-lived (ns) state formed in a side reaction, see discussion below).

In the blue-wavelength range the SADS of state E* is quite typical for a Chl excited state absorption spectrum.[36] The SADS of the P state in this wavelength range is very similar to that of the E state and resembles again the difference spectrum of a Chl excited state. It differs only at the short-wavelength end of the spectrum where this SADS goes negative. Such a signal is observed for example in the difference spectra of Chl cation radical states[36,37] (such a spectral contribution would indeed make sense since we propose a Chl/Chl CT character for the state P, see below). Clearly none of the two SADS in this model appears to be consistent with a Car state, neither an excited state nor a Car cation radical state.

Fitting the data with the slow/fast model (Figure 4) results in lifetimes which are, as expected, identical to those of the fast/slow model fit. Note that this slow/fast model corresponds essentially to the kinetic model proposed by Ruban et al.[20] in the absence of annihilation. While the SADS of the initial state (E*) looks similar to the one for the fast/slow model, that is, essentially those of a Chl excited state, the SADS of the P state (assigned to Lut1 S_1 in ref.[20]) looks very unusual. The most striking feature is the strong positive difference spectrum in the Q_y range (around 682 nm). Such a spectral shape can neither be explained with a Chl state nor is it consistent with a Car excited or radical state. This finding gives an initial hint that the "slow/fast" model (Figure 4) may correspond to that solution of the bi-exponential kinetics which is physically not reasonable, although the formal mathematical fit to the data is equally good as for the "fast/slow" model (Figure 3).

3. Discussion

Herein, the femtosecond transient absorption of in vitro LHC II oligomers was investigated to gain insight into the mechanism of energy dissipation that occurs upon oligomerization of LHC II. This in vitro aggregation of LHC II produces large energetically connected domains in which the excitations can migrate over many complexes.[38] Singlet–singlet annihilation in LHC II aggregates is a well-known phenomenon.[39–42] Compared to solubilized trimers, annihilation in aggregates occurs at much lower excitation intensities,[42] and in large systems it may take place on various timescales during the entire lifetime of the excited state(s), thus complicating extremely the observed relaxation kinetics. We therefore acquired the TA data under conditions where the probability for singlet–singlet annihilation is negligible. In consequence, the kinetics is simplified to the true intrinsic kinetics. This has the important effect that the number of rate constants required for describing the experimentally observed relaxation dynamics is drastically reduced as compared to high intensity excitation (see ref. [20]). This reduction in complexity allows us to reliably test relatively simple alternative kinetic models on the data.

3.1 Fast/Slow versus Slow/Fast Kinetic Models

The "slow/fast" model results in a large positive-amplitude SADS of the putative quencher state (P) in the Q_y range for both LHC II forms (Figure 4). Such a SADS cannot be produced by any potentially possible combination of Chl and/or Car states. Neither Chl excited states, Chl anions/cations, nor Lut excited states or quite generally Car cations/anions can produce such a signal. In the blue range, the SADS of the P state is negative, quite in contrast to what is expected for a Car S_1.[34] For comparison, the difference spectra of the Lut S_1 state—both in a solvent and in isolated LHC II monomers—are shown in Figure 4. Despite the small differences of the S_1 state spectrum in solvent and in intact LHC II, the discrepancy of these Lut S_1 SADS with the actual SADS of the P state in the slow/fast model is obvious. We can also exclude the possibility

of an electron-transfer process between Car and Chl[28] due to the absence of a negative-amplitude Car cation signal in the near-IR range (see Figure S3C of the Supporting Information); see also ref. [43] for relevant carotenoid cation difference spectra. Our kinetic analysis thus shows that only the "fast/slow" solution to the bi-exponential kinetic model leads to physically reasonable SADS (Figure 3), despite the fact that the "slow/fast" model (Figure 4) formally describes the data equally well.

There exists also a strong qualitative argument against a Car S_1 assignment of P as proposed by Ruban et al.[20] Such a model would require a fast rise term (negative-amplitude term with a lifetime of ca. 4–8 ps) in the Lut S_1 absorption range (520–560 nm). Such a rise term is clearly absent both in the LFD maps and in the original kinetic traces in the blue-wavelength range (Figure S5 of the Supporting Information). This rise term would be required to have the same absolute amplitude (but opposite sign) as the positive amplitude of the decay term of about 200 ps, which is a direct corollary of the kinetic reaction Scheme (see Supporting Information). Since the positive amplitude of the 200 ps component is easily detected in our data (Figure 2), it follows that we would also be able to resolve a negative amplitude component of similar absolute amplitude if it were present. Furthermore, the Lut1 S_1 quenching model[20] would also require a Lut S_1 character of the double difference spectrum $[\Delta A(30\text{ ps}) - \Delta A(500\text{ fs})]$ (see Figure S4 of the Supporting Information). This is also not the case.

The "fast/slow" model solution (Figure 3) in contrast results in SADS that are clearly physically meaningful. Both SADS can be interpreted in terms of Chl states both in the red as well as the blue wavelength ranges. Any evidence for the involvement of a carotenoid S_1 state is lacking. In the NIR range for this model again no evidence for the involvement of Car anions or cations is found. This excludes that a Car cation radical mechanism of the type proposed for quenching in minor LHCs[28,30] is active in LHC II aggregates. The data also show that the mechanism of singlet deactivation induced by oligomerization of LHC II does not require the presence of Zx, as follows from the nearly identical difference spectra and kinetics for the two LHC II forms. This finding is also in agreement with the results of our previous fluorescence studies.[17,41]

The SADS of the initially excited state E* (in both models) are typical of an excitonically coupled Chl excited state similar to those observed in reaction centers or excitonically coupled antenna systems.[36] The product, P, state's spectrum (in the "fast/slow" model) is similar to a Chl* spectrum. However, the bleaching of the P spectrum in the Q_y range reaches only about one third of the amplitude of the initially excited state E*. This indicates a correspondingly lower bleaching signal or - in this case of a SE - a lower radiative rate from that state. The SADS of the P state shows a broader bleaching spectrum in the Q_y range than the E* state and in particular it shows an increased tail of SE at the red end. Despite the dominating similarities in all samples and for all preparation conditions, the relative contribution of that red tail depends to some extent both on the preparation method of the aggregates and on the type of LHC II form. It is more pronounced in aggregates prepared by detergent dilution (Figure S7 of the Supporting Information) than with Bio-beads (Figure 3) and it is also slightly more pronounced for *npq2* LHC II than for *npq1*. For the same type of aggregate the red enhancement of the P state spectrum due to SE is generally somewhat smaller than in the fluorescence spectrum,[21] which is most likely due to overlap of the SE with some Chl excited state absorption (see Figure S4 of the Supporting Information for the development of the red SE signal) which partly compensates the negative-amplitude SE.

3.2 Proposed Quenching Mechanism

Comparison of the two investigated types of LHC II—from the *npq1* and *npq2* mutants of *A. thaliana*—revealed no significant differences in their behavior, both in terms of kinetics and TA spectra. In both LHC II types, the involvement of Chl to carotenoids energy transfer in the quenching can be excluded. It is clear that the P state in Figure 3 decays directly to the ground state of the system (ignoring the very small amount of triplet Chl formed) and only excited Chl states (showing GSB and SE in the visible range of the Qy transition) can explain the SADS of both model states. There exist no indications for the presence of further intermediates in our data. The relaxation of the S_1 state of Cars, particularly Lut, proceeds with a lifetime of about 10–15 ps both in solution[44] and when bound in LHC II.[34] A 200 ps transfer to the S_1 state followed by a 10 ps decay[20] would thus result in a 5% relative population of the S_1-excited Car. Considering that the difference molar absorption coefficient for the carotenoid S_1–S_n excited-state absorption (ESA) transition is very high (higher than the absorption coefficient of the Chl Q_y transition and similarly high as the strong ground state absorption of Cars), the involvement of a Car S_1 state would be clearly revealed in the data already qualitatively by a rise term in the Car wavelength range that should have at least 5% of the amplitude of the maximal Chl Q_y bleaching signal. However, the transient absorption in the blue region is about two orders of magnitude lower than the Q_y bleaching ($< 10^{-4}$ at 550 nm as compared to 10^{-2} for the bleaching at 682 nm, Figures 2C,D) and furthermore does not show any spectral features of a Car S_1 state absorption.

On the basis of the fluorescence kinetics and the spectral properties of the two fluorescent states that appear newly in LHC II aggregates as compared to LHC II trimers,[21] we suggested that the quenching process in oligomeric LHC II is solely due to Chl–Chl interactions. It is important to note here that this kinetic model (Figures 3C,D) describes not only the TA data presented here (Figures 3 A, B) but also the two Chl-like fluorescence components of LHC II aggregates with reasonable fluorescence SAES[21]). At the same time, the fluorescence data explicitly exclude the "slow/fast" model.[21] Thus the fast/slow model has much wider experimental support.

In our previous work, we intensely discussed the various possibilities for the assignment of the quenching state and came to the conclusion that it shows all the features of an emissive Chl exciton/CT state.[21] The SADS of Figure 3 appear to be in full agreement with such an interpretation. The actual

quenching of the initially excited Chl* states of LHC II in this mechanism occurs in two steps: In the first fast step (4–8 ps) a Chl excited state is trapped to a state assigned a Chl/Chl CT character. Such CT states can have an enhanced coupling to the ground state, which can lead to rapid direct recombination to ground state on a slower time scale of a few hundred ps, with a very small percentage forming a Chl triplet and/or Car triplet state. The formal kinetic description of this model, requiring two types of fluorescing Chl states, is well supported by the data (Figure 3). Furthermore, this is the only bi-exponential model that describes simultaneously the fluorescence and the TA kinetics while a model of energy transfer to a carotenoid S_1 state does neither describe the TA nor the fluorescence kinetics data. Note that both lifetimes show the signs of a pronounced distribution (Figure 2) which may indicate a heterogeneity in CT formation and decay kinetics in LHC II aggregates. Note that our present analysis averages both the kinetics and the spectra over this distribution since it is not possible to disentangle the closely overlapping lifetimes any further. It is possible that these distributions reflect some structural heterogeneity of the aggregates as has already been discussed in the corresponding fluorescence lifetime work.[21] Further work is necessary to provide final proof for the CT character of the intermediate state. Taking all present data into account we contend however that this remains the most likely assignment. A CT state could also explain well other previous data on LHC II oligomers, such as the spectrally broad low-temperature fluorescence emission above 700 nm[19,21,45] and the inefficiency of hole-burning in the long-wavelength absorption tail,[46] behavior that is also typical for the "red Chl" PSI antenna which has been assigned to a CT state on various grounds.[47,48] We also note that the CT character of the quenching state in LHC II aggregates has been tested earlier with conflicting results: While Pieper et al.[46] found evidence in favor of a CT character of the low energy forms this was questioned by Palacios et al.[49]

4. Conclusions

An important question and possible concern regarding the LHC II in vitro quenching model has been whether the quenching mechanism(s) operating in this system have any relevance for the in vivo NPQ quenching situation. This question has not been answered unequivocally so far. The results of this in vitro study lead to the conclusion that the quenching of the Chl singlet excitations in LHC II oligomers in vitro is neither dependent on Zx nor on energy transfer to any other Car (e.g. Lut1) but is solely a product of Chl–Chl interactions. This finding is at variance with the model of Ruban et al. involving the Lut1 S_1 state as an energy-transfer quencher.[20] We suggest that at present the most consistent interpretation of all available data is the formation of a fluorescent Chl/Chl CT state as intermediate in the quenching. Is this in vitro quenching mechanism also relevant for NPQ in vivo? We suggest, based on circumstantial evidence, that this is indeed the case. Our interpretation is supported by the long-wavelength-enhanced fluorescence emission component observed in LHC II oligomers.[21] An identical emission component that is strictly connected with NPQ conditions was discovered also in the ultrafast fluorescence kinetics of intact leaves of *Arabidopsis*.[21,22] All of these findings make it very likely that a situation very similar to that found in LHC II oligomers is actually formed in vivo in the NPQ process. How this is actually achieved in vivo is still an open question. Possible mechanisms would be the development of new Chl–protein interactions during NPQ either intra- or intermolecularly which could give rise to the formation of a Chl CT state quenching. We note that in vivo, one of the two resolved quenching processes does not require the involvement of Zx,[22] just as the CT-state formation in LHC II in vitro does not appear to require Zx.

Acknowledgements

This research was supported by the Deutsche Forschungsgemeinschaft (DFG, Sonderforschungsbereich SFB 663, Heinrich-Heine-Universität Düsseldorf and Max-Planck-Institute Mülheim a.d. Ruhr, Germany), and by the Netherlands Organization for Scientific Research (NWO)—Earth and Life Science (ALW) through a VIDI grant.

Keywords: carotenoids · femtochemistry · light-harvesting complex II · non-photochemical quenching · photosynthesis

[1] B. Demmig-Adams, W. W. Adams, *Nature* **2000**, *403*, 371–374.
[2] P. Horton, A. V. Ruban, *J. Exp. Bot.* **2005**, *56*, 365–373.
[3] K. K. Niyogi, X.-P. Li, V. Rosenberg, H.-S. Jung, *J. Exp. Bot.* **2005**, *56*, 375–382.
[4] A. V. Ruban, P. Horton, *Photosynth. Res.* **1994**, *40*, 181–190.
[5] A. R. Crofts, C. T. Yerkes, *FEBS Lett.* **1994**, *352*, 265–270.
[6] P. Horton, A. V. Ruban, R. G. Walters, *Annu. Rev. Plant Physiol. Plant Mol. Biol.* **1996**, *47*, 655–684.
[7] C. A. Wraight, A. R. Crofts, *Eur. J. Biochem.* **1970**, *17*, 319–327.
[8] J.-M. Briantais, C. Vernotte, M. Picaud, G. H. Krause, *Biochim. Biophys. Acta* **1979**, *548*, 128–138.
[9] G. Noctor, D. Rees, A. Young, P. Horton, *Biochim. Biophys. Acta* **1991**, *1057*, 320–330.
[10] B. Demmig-Adams, *Biochim. Biophys. Acta* **1990**, *1020*, 1–24.
[11] X.-P. Li, O. Björkman, C. Shih, A. R. Grossman, M. Rosenquist, S. Jansson, K. K. Niyogi, *Nature* **2000**, *403*, 391–395.
[12] S. Caffarri, G. Bonente, F. Passarini, S. Cazzaniga, M. Buia, R. Bassi, *Photosynth. Res.* **2007**, *91*, S157.
[13] K. K. Niyogi, *Annu. Rev. Plant Physiol. Plant Mol. Biol.* **1999**, *50*, 333–359.
[14] P. Müller, X.-P. Li, K. K. Niyogi, *Plant Physiol.* **2001**, *125*, 1558–1566.
[15] N. E. Holt, G. R. Fleming, K. K. Niyogi, *Biochemistry* **2004**, *43*, 8281–8289.
[16] A. V. Ruban, P. Horton, *Biochim. Biophys. Acta* **1992**, *1102*, 30–38.
[17] C. W. Mullineaux, A. A. Pascal, P. Horton, A. R. Holzwarth, *Biochim. Biophys. Acta* **1993**, *1141*, 23–28.
[18] P. Horton, A. V. Ruban, D. Rees, A. A. Pascal, G. Noctor, A. J. Young, *FEBS Lett.* **1991**, *292*, 1–4.
[19] A. V. Ruban, D. Rees, A. A. Pascal, P. Horton, *Biochim. Biophys. Acta* **1992**, *1102*, 39–44.
[20] A. V. Ruban, R. Berera, C. Ilioaia, I. H. M. van Stokkum, J. T. M. Kennis, A. A. Pascal, H. van Amerongen, B. Robert, P. Horton, R. van Grondelle, *Nature* **2007**, *450*, 575–578.
[21] Y. Miloslavina, A. Wehner, E. Wientjes, M. Reus, P. Lambrev, G. Garab, R. Croce, A. R. Holzwarth, *FEBS Lett.* **2008**, *582*, 3625–3631.
[22] A. R. Holzwarth, Y. Miloslavina, M. Nilkens, P. Jahns, *Chem. Phys. Lett.* **2009**, *483*, 262–267.
[23] P. Horton, M. Wentworth, A. V. Ruban, *FEBS Lett.* **2005**, *579*, 4201–4206.
[24] B. van Oort, A. van Hoek, A. V. Ruban, H. van Amerongen, *J. Phys. Chem. B* **2007**, *111*, 7631–7637.

[25] A. A. Pascal, Z. F. Liu, K. Broess, B. van Oort, H. van Amerongen, C. Wang, P. Horton, B. Robert, W. R. Chang, A. V. Ruban, *Nature* **2005**, *436*, 134 – 137.
[26] H. A. Frank, A. Cua, V. Chynwat, A. Young, D. Gosztola, M. R. Wasielewski, *Photosynth. Res.* **1994**, *41*, 389 – 395.
[27] H. A. Frank, J. A. Bautista, J. S. Josue, A. J. Young, *Biochemistry* **2000**, *39*, 2831 – 2837.
[28] N. E. Holt, D. Zigmantas, L. Valkunas, X.-P. Li, K. K. Niyogi, G. R. Fleming, *Science* **2005**, *307*, 433 – 436.
[29] T. K. Ahn, T. J. Avenson, M. Ballottari, Y.-C. Cheng, K. K. Niyogi, R. Bassi, G. R. Fleming, *Science* **2008**, *320*, 794 – 797.
[30] T. J. Avenson, T. K. Ahn, D. Zigmantas, K. K. Niyogi, Z. Li, M. Ballottari, R. Bassi, G. R. Fleming, *J. Biol. Chem.* **2008**, *283*, 3550 – 3558.
[31] K. K. Niyogi, A. R. Grossman, O. Björkman, *Plant Cell* **1998**, *10*, 1121 – 1134.
[32] S. Caffarri, R. Croce, J. Breton, R. Bassi, *J. Biol. Chem.* **2001**, *276*, 35924 – 35933.
[33] R. Croce, G. Canino, F. Ros, R. Bassi, *Biochemistry* **2002**, *41*, 7334 – 7343.
[34] R. Croce, M. G. Müller, R. Bassi, A. R. Holzwarth, *Biophys. J.* **2001**, *80*, 901 – 915.
[35] A. R. Holzwarth in *Biophysical Techniques in Photosynthesis. Advances in Photosynthesis Research* (Eds.: J. Amesz, A. J. Hoff), Kluwer Academic Publishers, Dordrecht, **1996**, pp. 75 – 92.
[36] A. R. Holzwarth, M. G. Müller, M. Reus, M. Nowaczyk, J. Sander, M. Rögner, *Proc. Natl. Acad. Sci. USA* **2006**, *103*, 6895 – 6900.
[37] D. C. Borg, J. Fajer, R. H. Felton, D. Dolphin, *Proc. Natl. Acad. Sci. USA* **1970**, *67*, 813 – 820.
[38] V. Barzda, G. Garab, V. Gulbinas, L. Valkunas, *Biochim. Biophys. Acta Bioenerget.* **1996**, *1273*, 231 – 236.
[39] T. Gillbro, A. Sandström, M. Spangfort, V. Sundström, R. van Grondelle, *Biochim. Biophys. Acta* **1988**, *934*, 369 – 374.
[40] T. Bittner, K.-D. Irrgang, G. Renger, M. R. Wasielewski, *J. Phys. Chem.* **1994**, *98*, 11821 – 11826.
[41] J. P. Connelly, M. G. Müller, M. Hucke, G. Gatzen, C. W. Mullineaux, A. V. Ruban, P. Horton, A. R. Holzwarth, *J. Phys. Chem. B* **1997**, *101*, 1902 – 1909.
[42] V. Barzda, V. Gulbinas, R. Kananavicius, V. Cervinskas, H. van Amerongen, R. van Grondelle, L. Valkunas, *Biophys. J.* **2001**, *80*, 2409 – 2421.
[43] S. Amarie, J. Standfuss, T. Barros, W. Kühlbrandt, A. Dreuw, J. Wachtveitl, *J. Phys. Chem. B* **2007**, *111*, 3481 – 3487.
[44] H. A. Frank, R. Z. B. Desamero, V. Chynwat, R. Gebhard, I. van der Hoef, F. J. Jansen, J. Lugtenburg, D. Gosztola, M. R. Wasielewski, *J. Phys. Chem. A* **1997**, *101*, 149 – 157.
[45] S. Vasil'ev, K.-D. Irrgang, T. Schrötter, A. Bergmann, H.-J. Eichler, G. Renger, *Biochemistry* **1997**, *36*, 7503 – 7512.
[46] J. Pieper, K.-D. Irrgang, M. Rätsep, T. Schrötter, J. Voigt, G. J. Small, G. Renk, R. Jankowiak, *J. Phys. Chem. A* **1999**, *103*, 2422 – 2428.
[47] R. Croce, A. Chojnicka, T. Morosinotto, J. A. Ihalainen, F. van Mourik, J. P. Dekker, R. Bassi, R. van Grondelle, *Biophys. J.* **2007**, *93*, 2418 – 2428.
[48] E. Romero, M. Mozzo, I. H. M. van Stokkum, J. P. Dekker, R. van Grondelle, R. Croce, *Biophys. J.* **2009**, L35 – L37.
[49] M. A. Palacios, R. N. Frese, C. C. Gradinaru, I. H. M. van Stokkum, L. L. Premvardhan, P. Horton, A. V. Ruban, R. van Grondelle, H. van Amerongen, *Biochim. Biophys. Acta Bioenerget.* **2003**, *1605*, 83 – 95.

Received: November 2, 2009
Published online on February 2, 2010

